Melt Viscosity–Molecular Weight Relationship for Linear Polymers

Ralph H. Colby[1]

Chemical Engineering Department, Northwestern University, Evanston, Illinois 60201

Lewis J. Fetters and William W. Graessley*

Exxon Research and Engineering Company, Corporate Research-Science Laboratories, Annandale, New Jersey 08801. *Received January 9, 1987*

ABSTRACT: The relationship between melt viscosity η_0 and molecular weight M for entangled linear polymers is accurately described by a power law, $\eta_0 \propto M^{3.4}$, up to $M/M_e \sim 150$, where M_e is the entanglement molecular weight. We have sought here to test the range of validity of that law by measurements on polymers with M/M_e as large as practically possible. Anionic polymerization was used to prepare a series of narrow distribution polybutadienes with low vinyl content and molecular weights ranging from 1×10^3 to 1.65×10^7 ($0.5 < M/M_e < 8000$). Several linear viscoelastic techniques were used to determine viscosities ranging from 1×10^0 P to 2×10^{12} P. Significant departures from the 3.4 power law were found beyond $M/M_e \sim 200$. The results are consistent with an approach to M^3 dependence as suggested by reptation theory, but the scatter is too large to allow a definite conclusion. The apparent η_0/M^3 asymptote is within a factor of 2 of a prediction based on reptation theory, modified by the contributions of tube renewal. Additionally, a comparison was made of the monomeric friction coefficient obtained from viscosities at low molecular weight and from transition responses at high molecular weight. Values of the modulus shift factor b_T were obtained for an unusually wide range of temperatures and are briefly discussed.

Introduction

The published data relating melt viscosity and molecular weight of entangled linear polymers can be described with considerable accuracy by a power law:

$$\eta_0 \propto M^{3.4} \qquad M > M_c \tag{1}$$

This form was first proposed in 1951 by Fox and Flory[2] on the basis of measurements on narrow distribution fractions of polystyrene and polyisobutylene. It has since been shown to apply to both melts and concentrated solutions for many species of flexible polymers.[3,4] The molecular weight M_c is a characteristic constant of the species in the melt state. Typically, $M_c \sim 2$–$3M_e$, where M_e is the entanglement molecular weight:[4]

$$M_e \equiv \rho RT/G_N^0 \tag{2}$$

in which ρ is the melt density, R is the gas constant, T is the temperature, and G_N^0 is the plateau modulus of the species. Sometimes the reported exponent is slightly different, but it is seldom less than 3.3 or more than 3.7. Equation 1 is supported by data that ranges up to 10–$20M_c$ for many species and as high as $50M_c$ in a few cases with no indication of systematic deviations.[3] There appears to be no data extending much beyond about $50M_c$, i.e., beyond $M/M_e \sim 150$.

However, acceptance of eq 1 as a limiting form leads to an apparent conflict with the seemingly well-established limiting forms for other properties of linear polymers, namely, the recoverable shear compliance,[4,5] the self-diffusion coefficient,[6-9] and the radius of gyration:[10]

$$J_e^0 \propto M^0 \qquad M \gtrsim 4M_c \tag{3}$$

$$D \propto M^{-2} \qquad M \gtrsim 3M_c \tag{4}$$

$$R_G \propto M^{1/2} \tag{5}$$

A simple calculation demonstrates the problem. The time for molecules to diffuse an average distance equal to their radius of gyration is

$$t_D = R_G^2/6D \tag{6}$$

Regardless of molecular structure or mechanism for chain mobility, it seems reasonable to expect orientational correlations in flexible polymers to disappear in a time of this order or less. The time scale for stress relaxation is[5]

$$\tau_0 = J_e^0\eta_0 \tag{7}$$

and this should correspond closely with the orientational relaxation time as measured, for example, by the decay of birefringence.[11] There are certainly situations in which orientation relaxes well before the chain moves a distance equal to its size—diffusion and stress relaxation in star polymers provide one example[12]—but the reverse situation, chains moving many R_G without orientational relaxation, seems extremely unlikely.

Accordingly, we expect

$$\Lambda = \frac{6J_e^0\eta_0 D}{R_G^2} < K \tag{8}$$

where K is a constant of order unity. (In the Rouse[4] and Doi–Edwards[13] models, for example, Λ is 2/5 and 6/5, respectively, while the experimental relationships for entangled star polymers[12] lead to $\Lambda \propto M^{-1}$.) However, eq 1 and 3–5 give $\Lambda \propto M^{0.4}$, and Λ is already of order unity for $M \sim 150M_e$ (for linear hydrogenated polybutadiene, see Figure 9 of ref 12). Thus, one or more of those equations must give way eventually to avoid inconsistency with eq 8 in the high molecular weight limit. If eq 8 is not obeyed we must then consider the possibility that diffusional and stress relaxation times obey different laws[14] or that memory of orientation can somehow persist during large chain displacements.

With such considerations in mind, we undertook to test eq 1 over the widest possible range of molecular weights and particularly up to the largest M/M_e that was experimentally feasible. Polybutadiene (~8% vinyl) was chosen for the study; availability via anionic polymerization (to give samples with narrow molecular weight distribution), low glass transition temperature ($T_g = -99$ °C, allowing the convenience and added accuracy of viscosity determinations near room temperature), and small entanglement spacing ($M_e = 1.85 \times 10^3$, based on a plateau modulus $G_N^0 = 1.20 \times 10^7$ dyn/cm^2)[15] make this polymer a species of choice for exploring the highly entangled regime.

0024-9297/87/2220-2226$01.50/0

Table I
Molecular Weight Data for Polybutadiene Samples

sample	$10^{-4}\bar{M}_n$(VPO)	$10^{-4}\bar{M}_n$(MO)	$10^{-4}\bar{M}_w$(LS)
CDS-B-2[a]	0.096		
C4[b]	0.17		
CDS-B-3[a]	0.23_5		
CDS-35[a]	0.27_6		
C7[b]	0.30		
C10[b]	0.42		
CDS-29[a]	0.63_8		
C17[b]	1.4_6		
C18		1.9_8	2.0_0
CDS-B-4[a]		2.2_6	2.3_6
CDS-30		4.5_7	
B1		6.8_1	7.0_9
C20		7.1_1	7.6_0
B2		$12._1$	$13._0$
B3		$35._5$	$35._5$
B4			$92._5$
B5			295
B6			374
B7			1650

[a] Characterization data supplied by Goodyear Chemicals. [b] Characterization data supplied by J. D. Tanzer, Northwestern University.

However, it must be carefully stabilized to prevent double bond reactions, and variations in microstructure must be minimized. Melt viscosities were measured for samples with molecular weights from $M \sim 10^3$ to $\sim 1.6 \times 10^7$, i.e., from $M/M_e \sim 5 \times 10^{-1}$ to $\sim 8 \times 10^3$. The data for low molecular weight samples were corrected for chain end effects (free volume) in order to evaluate M_c, to examine the iso-free volume form of $\eta_0(M)$ in the crossover region ($M \sim M_c$), and to obtain a numerical value of the monomeric friction coefficient. The data at high molecular weight were examined for departures from eq 1, and the results were compared with molecular theory. In the course of the work, we also obtained the modulus shift factor for viscoelastic response over an unusually wide range of temperatures. We briefly discuss that result as well.

Experimental Section

A. Polymerization. All samples were prepared by anionic polymerization in hydrocarbon solvents;[16] *sec*-butyllithium was the initiator, and degassed methanol or dry isopropyl alcohol was the terminating agent. Three series of samples were used. The B polymers were synthesized in 1:9 benzene–cyclohexane solutions under vacuum line conditions at 25 °C. Those samples were designed to cover the intermediate and the high ranges of molecular weight. The C polymers were synthesized in cyclohexane under nitrogen at 50 °C. Those samples cover the low molecular weight range, but they overlap extensively with the B series. A constant initiator concentration was used in the low range ($10^3 < M < 2 \times 10^4$) to minimize variations of chain microstructure. The CDS polymers are commercially available standard polybutadienes obtained from Goodyear. All samples were stabilized with small amounts of Ionol (Shell) or Santonox (Monsanto), added prior to precipitation from the polymerization solvent, and were stored in the dark and under vacuum until use.

B. Molecular Weight Determination. Molecular weights were obtained by vapor pressure osmometry (VPO) for several samples in the low molecular weight range ($M \lesssim 10^4$), by membrane osmometry (MO) for samples in the intermediate range ($10^4 \lesssim M \lesssim 3 \times 10^5$), and by low-angle laser light scattering (LS) for samples in the intermediate and high ranges ($10^4 \lesssim M$). Membrane osmometry and light scattering procedures are described in Appendix A. The results, given in Table I, were used to construct the calibration curve for size exclusion chromatography (SEC) shown in Figure 1.

The SEC measurements were made at 25 °C with a Waters 150-C instrument using μ-Styragel columns and tetrahydrofuran as the elution solvent. Four well-characterized samples (CDS-B-2, CDS-B-3, CDS-29, and C18) were used as low M standards, and the molecular weights for other samples in that range were obtained from the resulting SEC calibration. The molecular weights reported in the tables for $M < 2 \times 10^4$ are SEC values of $\bar{M}_w$ (essentially the elution peak values). The SEC calibration for higher molecular weights (up to $M \sim 10^6$, the "good" resolution limit for our column set) was established with the $\bar{M}_w$ (LS) data in Table I. The result was used as a check of internal consistency for those molecular weights and to obtain values of $\bar{M}_w$ (SEC) for a few other samples. Molecular weights given in tables for $M > 2 \times 10^4$ are $\bar{M}_w$ (LS) when those were measured and $\bar{M}_w$ (SEC) otherwise. Values of $\bar{M}_w/\bar{M}_n$ were estimated from the elution curves; only samples with $\bar{M}_w/\bar{M}_n < 1.1$ (uncorrected for column dispersion) and free of high and low molecular weight tails were used in the rheological studies. Beyond $M = 10^6$, there is only indirect (rheological) evidence about sample polydispersity, as will be discussed below.

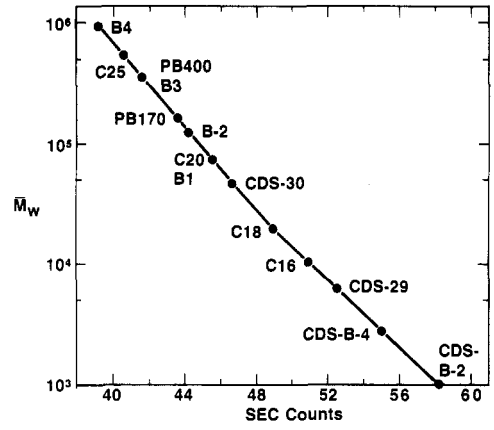

Figure 1. Calibration curve for size exclusion chromatography of polybutadiene in tetrahydrofuran.

Table II
Intrinsic Viscosity of Polybutadiene Samples

sample	$10^{-4}M$	$[\eta]_{THF}$	$[\eta]_{CHN}$
C18	2.00	0.421	0.393
CDS-30	4.60		0.692
B1	7.09	1.03	0.926
C20	7.60	1.09	
B2	13.0	1.62	1.424
B3	35.5	3.37	2.96
C25	54.8	4.41	3.85
B4	92.5	6.40	5.67
B5	295	14.5	
B6	374	17.9	14.5
B7	1650	46.0	

Intrinsic viscosity $[\eta]$ was measured at 25 °C in tetrahydrofuran for all high molecular weight samples and in cyclohexane for selected samples, the purpose being to provide another smoothness test of internal consistency for the molecular weights. Values in tetrahydrofuran were determined at several shear rates for the four samples of highest molecular weight (B4, B5, B6, and B7). Except for sample B7, the zero shear rate limit for $[\eta]$ was reached in the experimental range. Extrapolation was required for B7; the zero shear rate limit for that sample was obtained by a reduced variables procedure based on dilute solution theory and data for the other samples.[17] The results are given in Table II and plotted as a function of molecular weight in Figure 2. Results were omitted for B5 (abnormal vinyl content, see below) and B7 (uncertainty due to shear rate dependence). The remaining data are accurately described by Mark–Houwink–Sakurada equations

$$[\eta] = 3.53 \times 10^{-4} M^{0.715} \quad (\text{dL g}^{-1}, \text{tetrahydrofuran}) \qquad (9)$$

$$[\eta] = 4.09 \times 10^{-4} M^{0.693} \quad (\text{dL g}^{-1}, \text{cyclohexane}) \qquad (10)$$

with correlation coefficients of 0.9999 in each case.

C. Chemical Microstructure. Microstructural information was obtained by Fourier transform infrared spectroscopy (FTIR) (Digilab FTS 15-E) and proton nuclear magnetic resonance (NMR) (JEOL GX-400). Standard procedures were used for

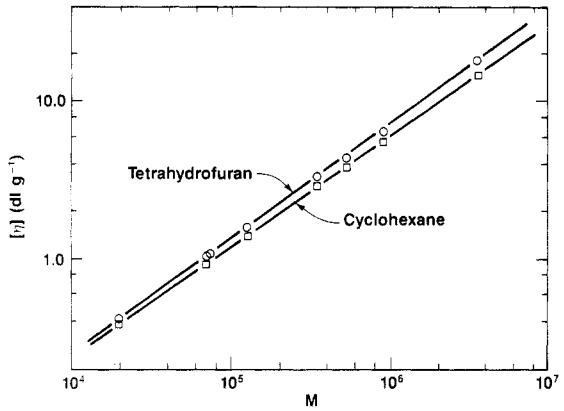

Figure 2. Intrinsic viscosity for polybutadiene in tetrahydrofuran and cyclohexane. The lines are given by eq 9 and 10 in the text.

Table III
Chemical Microstructure of Polybutadiene Samples

sample	M	% 1,4 cis	% 1,4 trans	% 1,2 (vinyl)
CDS-B-2	1.03×10^3	29 (36)[a]	53 (49)[a]	18 (15)[a]
C1	1.13	$33._5$	58	$8._5$
C2	1.19	$33._5$	$56._5$	10
C3	1.42	34	58	8
C5	2.12	34	58	8
C6	2.57	35	57	8
C8	3.73	35	56	9
C9	4.03	35	57	8
C11	4.43	34	$57._5$	$8._5$
C12	5.96	35	$56._5$	$8._5$
CDS-29	6.29	$35._5$ (36)	56 (55)	$8._5$ (9)
C14	6.95	34	57	9
C16	1.05×10^4	35	$56._5$	$8._5$
C18	2.00	36	55	9
CDS-B-4	2.6	36 (40)	$55._5$ (52)	$8._5$ (8)
C19	3.8	36 (38)	56 (54)	8 (8)
CDS-30	4.60	$34._5$ (40)	57 (50)	$8._5$ (10)
B1	7.09	37 (40)	54 (51)	9 (9)
C20	7.60	39	53	8
B2	1.30×10^5	$35._5$ (41)	$54._5$ (50)	10 (9)
C22	1.9	$38._5$ (44)	$53._5$ (49)	8 (7)
C23	2.1	$42._5$	50	$7._5$
B3	3.55	40 (47)	51 (45)	9 (8)
C24	4.3	43	50	7
C25	5.48	43 (52)	50 (41)	7 (7)
B4	9.25	45 (50)	46 (42)	9 (8)
B5	2.95×10^6	39 (44)	46 (43)	15 (13)
B6	3.74	57 (59)	35 (34)	7 (7)
B7	1.65×10^7	(66)	(25)	(9)

[a] Values in parentheses obtained by NMR; other values obtained by FTIR.

calibration and operation;[17] the proportions of cis-1,4, trans-1,4, and 1,2 (vinyl) additions determined from these measurements are given in Table III. Agreement between the two methods is generally good. The vinyl content lies between 7% and 9%, the only significant exceptions being sample CDS-B-2 with ~16% vinyl units and sample B5 with ~14% vinyl units. The glass transition temperature T_g varies with vinyl content,[18,19] and constancy of T_g is crucial in η_0–M comparisons. The cis–trans ratio is roughly 35/57 below $M \sim 10^5$, but it then drifts upward, reaching 66/25 for sample B7 at $M = 1.65 \times 10^7$. This trend has been noted by others[16] and is related to the reduced active center concentration used when preparing polymers of high molecular weight. The cis–trans ratio does not affect T_g significantly (except perhaps at very high (>80%) trans content),[18] and its influence on melt viscosity appears to be small, as discussed below.

D. Density and Glass Transition Temperature. Both density, ρ, and glass transition temperature, T_g, vary linearly with the chain end concentration ($\propto M^{-1}$).[3] Density measurements were made at 25 and 60 °C on several samples in the low molecular weight range with a Mettler Density Meter. Those results and thermal expansion coefficients, calculated as $\alpha = -\Delta \ln \rho / \Delta T$, are given in Table IV. The molecular weight dependences are well described by

Table IV
Glass Transition and Density Data for Polybutadiene Samples

sample	M	T_g (K)	ρ (g/cm³) at 25 °C	ρ (g/cm³) at 60 °C	$10^4\alpha$ (K⁻¹)
C1	1.13×10^3	163.3	0.874_6	0.852_5	7.5_5
C2	1.19	163.5	0.875_4	0.853_5	7.4_7
C3	1.42	166.4	0.879_0	0.857_1	7.4_4
C5	2.12	168.1	0.883_5	0.861_8	7.3_3
C6	2.57	170.2			
C8	3.73	171.5	0.887_5	0.866_1	7.1_9
C9	4.03	170.5			
C12	5.96	171.7			
C13	6.10		0.890_8	0.869_1	7.0_9
CDS-29	6.29	173.7			
C16	1.05×10^4		0.892_2	0.871_0	7.0_8
C19	3.8	173.7			
CDS-30	4.60	175.3			
B1	7.09	174.8			
C20	7.60	176.3			
B2	1.30×10^5	175.0			
B3	3.55	175.4			
C25	5.48	172.1			
B4	9.25	174.2			
B5	2.95×10^6	178.2			
B6	3.74	171.9			
B7	1.65×10^7	172.1			

$$1/\rho = 1.118 + 30.9/M \quad (\text{cm}^3\ \text{g}^{-1},\ 25\ ^\circ\text{C}) \tag{11}$$

$$\alpha = 7.0 \times 10^{-4} + 0.06/M \quad (\text{K}^{-1}) \tag{12}$$

The density obtained from the large M intercept, $\rho = 1/1.118 = 0.894_5$ g cm^{-3}, agrees well with $\rho = 0.895$ at 25 °C obtained for one high molecular weight sample (C25) by a neutral buoyancy method and 0.896 reported elsewhere.[18] The thermal expansion coefficient obtained from the large M intercept, $\alpha = 7.0 \times 10^{-4}$ K^{-1}, is slightly smaller than a reported value of 7.5×10^{-4} K^{-1} for this microstructure.[20]

The glass transition temperature, T_g, was determined for many samples with a differential scanning calorimeter (Perkin-Elmer DSC-2). Samples were first quenched to 140 K and then temperature was scanned up at rates of 5, 10, and 20 °C/min. The midpoint temperature of the heat capacity transition was extrapolated to zero heating rate, providing the values of T_g reported in Table IV. Results for the low molecular weight samples are well fitted by

$$T_g = 174 - 12100/M \quad (\text{K}) \tag{13}$$

The large M intercept, $T_g = 174$ K, lies in the midst of values obtained for the high molecular weight samples ($M > 10^4$) except for sample B5 whose T_g is higher by 4 K, in agreement with expectations based on its somewhat elevated vinyl content.[19] Variability in T_g among the other high molecular weight samples is larger than our reproducibility estimate of ±0.5 K and in most cases seems to correlate with the ±1% variations in 1,2 content of the samples. Little effect of cis–trans ratio is seen, with the possible exception of sample B7 where T_g is ~2 K below the value expected from its vinyl content.

E. Rheology. Viscosities ranging from ~0.2 to $\sim 2 \times 10^{12}$ P were determined in the course of this work. Four methods were used—gravity-driven flow in capillary viscometers (2×10^{-1} P < $\eta_0 < 4 \times 10^3$ P), oscillatory shear flow in a parallel plate rheometer (1×10^0 P < $\eta_0 < 5 \times 10^8$ P), stress relaxation in a parallel plate rheometer (3×10^7 P < $\eta_0 < 5 \times 10^{10}$ P), and creep compliance in a creep rheometer (4×10^8 P < $\eta_0 < 2 \times 10^{12}$ P). Measurements were made for a wide range of temperatures on several samples to gather the information necessary to correct the viscosity of low molecular weight samples for chain end (free volume) differences. Measurements on low molecular weight samples at low temperature were limited by the onset of crystallization below −30 °C.[21] High molecular weight samples ($M > 5 \times 10^4$) did not crystallize, and data were obtained for one sample down to −91 °C (within

Table V
Kinematic Viscosity Data for Low Molecular Weight Polybutadiene Samples from Capillary Viscometry

sample	$10^{-3}M$	ν (St) at 0 °C	25 °C	50 °C	75 °C
CDS-B-2	1.03	4.02	1.13	0.460	0.236
C1	1.13	4.12	1.24	0.527	0.274
C2	1.19	4.26	1.28	0.537	0.278
C3	1.42	7.12	2.06	0.837	0.428
C4	1.60		2.22		
C5	2.12	14.8	4.07	1.60	0.786
C6	2.57	20.9	5.67	2.18	1.066
C7	3.30		6.39		
C8	3.73	40.9	10.8	4.06	1.94
C9	4.03	50.8	13.3	4.99	2.37
C10	4.50		19.7		
C11	4.43	74.3	19.1	7.09	3.35
C12	5.96	145	37.0	13.7	6.44
C13	6.10	158	40.0	14.7	6.79
CDS-29	6.29		47.9	17.6	8.18
C14	6.95	227	57.1	20.6	9.60
C15	8.50		75.6		
C16	10.5		184	66.3	30.2
C18	20.0		2400	849	385
CDS-B-4	25.0		3740		

8 °C of T_g). Experimental procedures and the analysis of temperature dependence are summarized below.

1. Capillary Viscometry. Viscosity for the low molecular weight samples ($M < 3 \times 10^4$) was measured with calibrated Cannon-Ubbehlode glass capillary viscometers (Cannon Instrument Company) equipped with automatic timers. Kinetic energy and shear rate effects were negligible. Kinematic viscosity, $\nu = \eta_0/\rho$, was obtained at several temperatures for many samples; results are given in Table V.

2. Oscillatory Shear Rheometry. The complex shear modulus, $G^*(\omega) = G'(\omega) + iG''(\omega)$, was measured for a wide range of frequencies ($10^{-4} < \omega < 10^2$ s^{-1}) on many samples and at several temperatures with a Rheometrics System Four rheometer. The parallel plate geometry was used—25-mm diameter platens when $|G^*|$ was less than 10^7 dyn/cm^2 throughout the run and 7.9-mm platens for higher moduli. The smaller platens were used to minimize effects caused by the torsional compliance of the instrument; errors from this source should be small for $|G^*| < 10^{10}$ dyn/cm^2.[22] Platens with 50-mm diameter were used for low molecular weight samples. Samples of high molecular weight were compression molded under vacuum and trimmed to shape after mounting. As described elsewhere,[23] linearity of response was confirmed repeatedly, and careful account was taken of dimensional changes with temperature. Viscosity was obtained from[4]

$$\eta_0 = \lim_{\omega \to 0} \frac{G''(\omega)}{\omega} \tag{14}$$

and, in some high molecular weight samples, from[4]

$$\eta_0 = \frac{2}{\pi} \int_{-\infty}^{\infty} \frac{G'(\omega)}{\omega} \, d \ln \omega \tag{15}$$

Viscosities obtained from eq 14 are given in Tables VI and VII. Values obtained from eq 15 agreed within a few percent when sufficient data were available to perform the numerical integration. Moreover, the form of $G'(\omega)/\omega$ vs. ln ω was found to be invariant in the high molecular weight range (judged by data for samples B1–B4 at various temperatures), such that eq 15 translates to a simple relationship between viscosity and the peak value of $G'(\omega)/\omega$ in the terminal region:[17]

$$\eta_0 = 2.21[G'(\omega)/\omega]_{max} \tag{16}$$

This equation was used to estimate η_0 for sample B5 at 73 °C where the data at low frequencies were insufficient to apply either eq 14 or 15. The "best" values of η_0 for high molecular weight samples from eq 14–16 are listed under $G^*(\omega)$ in Table VIII.

3. Shear Stress Relaxation. The Rheometrics System Four rheometer and parallel plate geometry were also used to determine the shear stress relaxation modulus $G(t)$ for four high molecular weight samples (B3–B6). Poor adhesion to the platens proved to be a problem for samples B5 and B6. Several methods to improve the adhesion were tested. Satisfactory results were finally achieved by attaching the polymer sheet to the platens with a thin layer of cyanoacrylate adhesive. Small steps in torsional displacement were applied; linearity of response was confirmed by comparing measurements of torque vs. time for a range of displacements. No indication of abnormal sensitivity to strain was found even in the samples of highest molecular weight. Data from clockwise and counterclockwise steps were averaged to minimize the effects of transducer drift. The results were converted to stress relaxation modulus, $G(t)$, and viscosity was calculated from[4]

$$\eta_0 = \int_{-\infty}^{\infty} tG(t) \, d \ln t \tag{17}$$

Values obtained by numerical integration are listed under $G(t)$ in Table VIII.

4. Shear Creep Compliance. Creep compliance $J(t)$ was measured at 22 °C for three of the high molecular weight samples (B4, B6, and B7) with a Magnetic Elevation Creep Apparatus (MECA) by D. L. Plazek of Time–Temperature Instruments, Inc. The procedures have been described elsewhere.[24] Samples were molded into sheets as described above. Viscosity was obtained from[4]

$$\eta_0 = \lim_{t \to \infty} (t/J(t)) \tag{18}$$

Steady-state creep was achieved for samples B4 and B6 but not for sample B7, even after ~4 days. For the latter sample, η_0 was obtained by the Ninomiya extrapolation method,[25] the value agreeing within 3% with the last measured value of $t/J(t)$. The results are listed under $J(t)$ in Table VIII.

F. Temperature Dependence. Time–temperature superposition was found to apply for the dynamic modulus data obtained here. Thus,[4]

$$G^*(\omega;T) = b_T G^*(a_T\omega;T_0) \tag{19}$$

where a_T and b_T are frequency and modulus shift factors with respect to a reference temperature T_0 ($a_T \equiv 1$ and $b_T \equiv 1$ at T_0). We used $T_0 = 25$ °C for all samples. Values of a_T and b_T obtained

Table VI
Shear Viscosity Data for Low Molecular Weight Polybutadiene Samples from Oscillatory Rheometry

sample	η_0 (P) at −30 °C	−28 °C	−8 °C	−6 °C	−2 °C	25 °C	49 °C
C3		60.2			7.70	1.81	
C5		113			15.2	3.66	
C6						4.82	
C8	460		56.9			9.65	
C9	471		64.7			12.0	
C11		590			74	16.3	6.37
C12	1 240			178		34.0	
C13		1300			159		13.1
CDS-29		1600			188	40.5	16.4
C14		1910			235	50.0	18.5
C16	7 000			895		171	60.9
C18	118 000		14 400			2150	790

Table VII
Viscoelastic Properties of High Molecular Weight Polybutadiene Obtained from Dynamic Modulus Measurements

sample	T (°C)	η_0 (P)	G_m'' (dyn/cm^2) × 10^{-6}	log a_T	b_T
CDS-30	−51		2.15	2.99	0.81
(M = 4.60 × 10^4)	−26	1.22 × 10^6	2.33	1.60	0.88
	0	1.54 × 10^5	2.52	0.66	0.95
	25	3.53 × 10^4	2.66	0	1.00
	48	1.40		−0.42	
	73	5.9 × 10^3		−0.81	
B1	−51	1.09 × 10^8	2.46	3.01	0.78
(M = 7.09 × 10^4)	−26	4.75 × 10^6	2.70	1.61	0.86
	0	5.96 × 10^5	2.96	0.67	0.94
	25	1.36	3.14	0	1.00
C20	−76			5.32	
(M = 7.60 × 10^4)	−51[b]		2.08	2.92	0.79
	−51[b]		2.11	2.91	0.80
	−26	4.95 × 10^6	2.27	1.52	0.86
	0	6.75 × 10^5	2.49	0.62	0.94
	25	1.73	2.65	0	1.00
B2	−91			8.53	0.72 (0.66)[a]
(M = 1.30 × 10^5)	−86			7.23	0.74 (0.68)[a]
	−81			6.28	0.75 (0.69)[a]
	−76			5.59	0.78 (0.72)[a]
	−51			2.93	0.86 (0.79)[a]
	−26	3.65 × 10^7	2.65	1.56	0.86
	0	5.01 × 10^6	2.88	0.66	0.94
	25	1.20	3.07	0.00	1.00
	48	4.72 × 10^5	3.31	−0.44	1.08
	73	2.18	3.45	−0.80	1.12
	100	1.19	3.55	−1.07	1.16
	125	7.31 × 10^4	3.64	−1.30	1.19
B3	25	3.12 × 10^7	3.37	0	1.00
(M = 3.55 × 10^5)	48	1.17	3.50	−0.44	1.04
	73	5.37 × 10^6	3.60	−0.79	1.07
B4	25	4.48 × 10^8	3.55	0	1.00
(M = 9.25 × 10^5)	47	1.76	3.71	−0.42	1.05
	73	8.5 × 10^7	3.82	−0.75	1.08

[a] The apparent values of b_T obtained for sample B2 are believed to be too large because of a small error in gap setting (the 7.9-mm platens used at −51 °C and below and the 25-mm platens at −26 °C and above). The values in parentheses are corrected downward by 9%, to make b_T at −51 °C agree with b_T at −51 °C for sample C20. [b] First entry for −51 °C obtained with 7.9-mm platens, second entry with 25-mm platens.

Table VIII
Viscosity of High Molecular Weight Polybutadiene Samples from Loss Modulus, Stress Relaxation, and Creep Compliance

		η_0 (P)		
sample	at T (°C)	from $G^*(\omega)$	from $G(t)$	from $J(t)$
B3	25	3.12 × 10^7	2.92 × 10^7	
(M = 3.55 ×	48	1.17	1.10	
10^5)	73	5.38 × 10^6	5.11 × 10^6	
B4	22	(5.15 × 10^8)[a]	(5.05 × 10^8)[a]	5.0 × 10^8
(M = 9.25 ×	25	4.48 × 10^8	4.40 × 10^8	
10^5)	48	1.76	1.65	
	73	8.56 × 10^7	7.99 × 10^7	
B5	25		2.0 × 10^{10}	
(M = 2.95 ×	73	4.0 × 10^9	4.0 × 10^9	
10^6)				
B6	22		(5.9 × 10^{10})[b]	6.6 × 10^{10}
(M = 3.74 ×	25		4.4 × 10^{10}	
10^6)	73		9.0 × 10^9	
B7	22			2.2 × 10^{12}
(M = 1.65 ×				
10^7)				

[a] Estimated from value at 25 °C with a_{22} = 1.16 from eq 19 with C_1 = 3.48 and C_2 = 163 K and with b_{22} = 0.99 from Table IX. [b] Estimated from value at 73 °C with a_{22}/a_{73} = 7.18 from eq 19 with C_1 = 3.48 and C_2 = 163 K and with b_{22}/b_{73} = 0.91 from Table IX.

for several samples are listed in Table VII. Master curves of $G'(\omega)$ and $G''(\omega)$ for sample B2 are shown in Figure 3. The apparent glassy modulus, $G_g \sim 2 \times 10^9$ dyn/cm^2, is much smaller than values found for other polymers[4] as well as a result of $\sim 10^{10}$ dyn/cm^2 obtained for polybutadiene networks.[26] Our low result probably indicates some sample slippage at high frequencies and

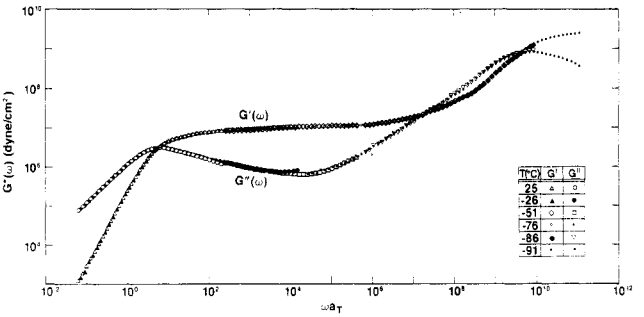

Figure 3. Dynamic modulus master curves for sample B2 (M = 1.30 × 10^5) at the reference temperature T_0 = 25 °C.

Table IX
Average Values of Modulus Shift Factor for Polybutadiene (Reference Temperature T_0 = 25 °C)

T (°C)	b_T	no. of samples	T (°C)	b_T	no. of samples
−91	0.66	1	0	0.94	4
−86	0.68	1	25	1.00	all
−81	0.69	1	48	1.06	3
−76	0.69	2	73	1.09	3
−51	0.80	3	100	1.16	1
−26	0.86	4	125	1.19	1

low temperatures ($|G^*| \gtrsim 3 \times 10^8$ dyn/cm^2).

The modulus shift factor changes very slowly with temperature, but values of b_T can still be obtained with reasonable accuracy from variations of the terminal loss peak G_m'' (Table VII) when the loss peak frequency ω_m is in the experimental range.[23] Other modulus benchmarks provide some guidance in the plateau and transition regions. Good agreement among the samples was found;

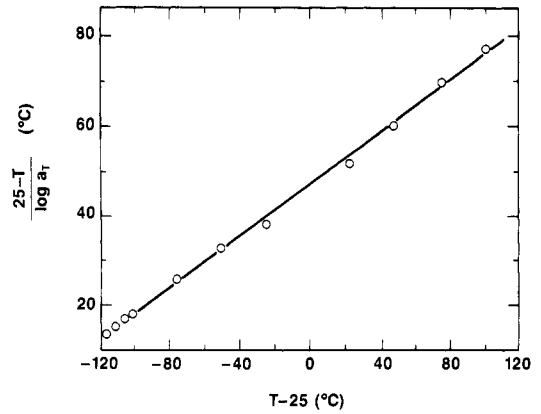

Figure 4. WLF plot of the frequency shift factor for sample B2 with T_0 = 25 °C. The line is given by eq 20 with C_1 = 3.48 and C_2 = 163 K.

Table X
WLF Coefficients and Free Volume Parameters for Polybutadiene Samples

sample	$10^{-3}M$	C_1[a]	C_2 (K)[a]	ζ^∞/ζ^b	ν_∞ (St)[c]
CDS-B-2	1.03	2.69	147	6.08	6.88
C1	1.13	2.66	153	6.46	8.03
C2	1.19	2.74	156	5.47	7.01
C3	1.42	2.80	155	4.74	9.77
C5	2.12	2.94	156	3.42	13.9
C6	2.57	3.00	157	2.97	16.9
C8	3.73	3.14	161	2.16	23.3
C9	4.03	3.12	159	2.24	29.7
C11	4.43	3.18	160	1.99	38.1
C12	5.96	3.18	159	1.96	72.6
C13	6.10	3.23	160	1.75	70.0
CDS-29	6.29	3.22	160	1.81	86.6
C14	6.95	3.29	162	1.53	87.2
C16	10.5	3.43	168	1.11	205
C18	20.0	3.33	159	1.39	3350
B2	130	3.48	163	(1.0)	

[a] Reference temperature T_0 = 25 °C for all samples. [b] Monomeric friction coefficient for high molecular polybutadiene at 25 °C divided by the value for each of the samples as determined by the method described in Appendix B. [c] Kinematic viscosity, corrected to the fractional free volume of high molecular weight polybutadiene at 25 °C.

the averages of values obtained for b_T at various temperatures are given in Table IX.

The temperature dependence of a_T for many species of flexible polymers is accurately described by the WLF equation[4]

$$\log a_T = -\frac{C_1(T - T_0)}{C_2 + T - T_0} \tag{20}$$

where C_1 and C_2 are independent of molecular weight for large M. Figure 4 shows a WLF plot of the data for sample B2. Values of a_T from −91 to 125 °C for that sample are well represented by eq 20 with C_1 = 3.48 and C_2 = 163 K which describes results for the other high molecular weight samples (Table VII) as well.

Viscosity data are available over a range of temperatures for the low molecular weight samples, and according to the superposition principle[27]

$$\eta_0(T) = a_T b_T \eta_0(T_0) \tag{21}$$

Since b_T depends so weakly on temperature, its variation can be safely ignored to obtain the frequency shift factors simply from the viscosity ratios:

$$a_T = \eta_0(T)/\eta_0(T_0) \tag{22}$$

Values of a_T so obtained from the data in Table V (T_0 = 25 °C) are also accurately described by WLF equations but with C_1 and C_2 that vary systematically with molecular weight. The values in Table X were determined from capillary flow data alone (Table V) because temperature accuracy and control was better for those measurements (±0.1 °C) than in the oscillatory instrument (±1.0 °C). Results from the latter (Table VI) are consistent with the capillary results but somewhat more scattered.

Table XI
Viscosity of Polybutadiene Samples at 25 °C with and without Correction to Constant Free Volume

sample	M	η_0 (P)	$(\eta_0)_\infty$ (P)[a]
CDS-B-2	1.03×10^3	0.99	6.0
C1	1.13	1.08	7.0
C2	1.19	1.12	6.1
C3	1.42	1.8	8.5
C5	2.12	3.56	1.22×10^1
C6	2.57	5.0	1.49
C8	3.73	9.5	2.05
C9	4.03	1.18×10^1	2.6
C11	4.43	1.7	3.4
C12	5.96	3.3	6.5
C13	6.10	3.6	6.3
CDS-29	6.29	4.3	7.7
C14	6.95	5.1	7.8
C16	1.05×10^4	1.67×10^2	1.83×10^2
C18	2.00	2.15×10^3	
CDS-30	4.60	3.53×10^4	
B1	7.09	1.33×10^5	
C20	7.60	1.73	
B2	1.30×10^5	1.21×10^6	
B3	3.55	3.0×10^7	
B4	9.25	4.4×10^8	
B5	2.95×10^6	2.0×10^{10}	
B6	3.74	5.7	
B7	1.65×10^7	1.9×10^{12}	
PB170	1.64×10^5	2.26×10^6	
PB400	3.61	3.18×10^7	
C19	3.68×10^4[b]	1.35×10^4	
M1	9.28[b]	3.13×10^5	
M2	1.00×10^5[b]	4.37	
C22	1.68[b]	2.95×10^6	
M3	4.41[b]	4.97×10^7	

[a] Melt viscosity corrected to constant monomeric friction coefficient as described in Appendix B. For higher molecular weights, $(\eta_0)_\infty = \eta_0$. Viscosity-average molecular weight calculated from the intrinsic viscosity in tetrahydrofuran (eq 9), $[\eta]$ = 0.65, 1.26, 1.33, 1.93, and 3.84 dL g^{-1}, respectively.

Results and Discussion

A. Melt Viscosity–Molecular Weight Relationship. Viscosities at 25 °C for all samples are listed together with molecular weights in Table XI. Also included are data obtained in our laboratory for two samples kindly provided to us by Roovers (PB170 and PB400)[28] and data for five samples measured previously by Struglinski (C19, M1, M2, C22, and M3).[15] The light-scattering molecular weights reported by Roovers agree closely with our SEC estimates for his samples. Molecular weights were calculated for the Struglinski samples from $[\eta]$ in tetrahydrofuran with eq 9. The viscosities of the low molecular weight samples were adjusted to the free volume state of high molecular samples at 25 °C, as described below and in Appendix B.

The accuracy of viscosity measurement for the samples of highest molecular weight (B3–B7) is of course crucial to this work. Values of η_0 at 25 °C were obtained from the results of various methods (Table VIII). For sample B3, we simply used the average of values from $G^*(\omega)$ and $G(t)$ at 25 °C. For sample B4, we used the average of values from $G^*(\omega)$ and $G(t)$ at 25 °C and from $J(t)$ at 22 °C, adjusted to 25 °C with eq 21 (a_{22} = 1.16, b_{22} = 0.99). The three values differed by no more than 3%, as can be seen in Table VIII. For sample B5, we used only the value from $G(t)$ at 25 °C, the shift factors for 73 °C being uncertain because B5 has an elevated vinyl content. Three values were obtained from sample B6—4.4×10^{10} P from $G(t)$ at 25 °C, 5.0×10^{10} P from $G(t)$ at 73 °C after adjustment to 25 °C (a_{73} = 0.162, b_{73} = 1.09), and 5.7×10^{10} P from

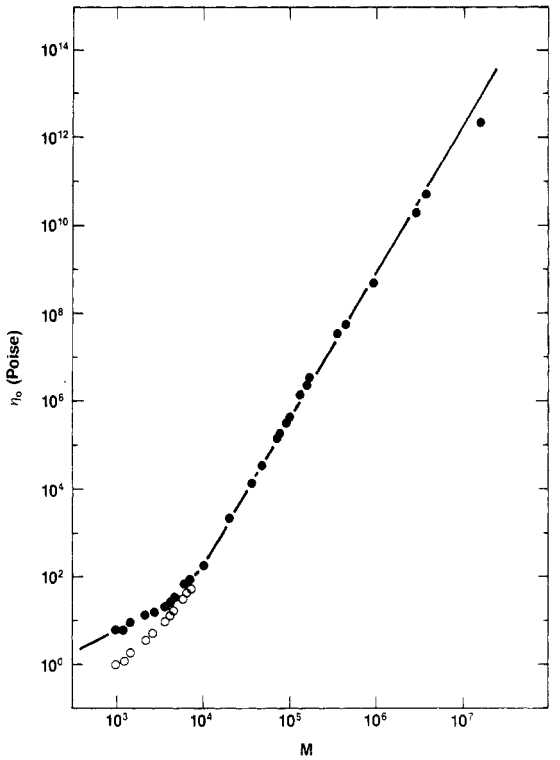

Figure 5. Viscosity vs. molecular weight for polybutadiene at 25 °C. The filled circles indicate data at the iso-free-volume state; the open circles indicate the unadjusted results (see Table XI). The lines have been drawn with slopes of 1.0 and 3.4.

$J(t)$ at 22 °C after adjustment to 25 °C. We used the value from $J(t)$ because the measurements still lie well within the capability of the MECA instrument but are at the limit of the System Four. For sample B7, we have only the extrapolated value from $J(t)$, adjusted to 25 °C.

The results for all samples are plotted in Figure 5, and broadly speaking, they follow the familiar power law pattern with an exponent that is near unity for low molecular weight samples (after the adjustment to constant free volume) and near 3.4 for high molecular weight samples. The behavior in each regime is examined in more detail below.

1. Low Molecular Weight Polymers. Kinematic viscosities at 25 °C (Table V) were adjusted to constant monomeric friction coefficient (corresponding to that for high molecular weight samples at 25 °C) by the method described in Appendix B. The correction factor ζ^∞/ζ and the adjusted kinematic viscosity ν_∞ are listed in Table X. Values of ν_∞ in the low molecular weight range are plotted in Figure 6. The data define a smooth curve going to $\nu_\infty \propto M^{3.41}$ for long chains (up to $M \sim 4 \times 10^5$ as discussed below). The results in Figure 6 are well described by

$$\nu_\infty = 6.49 \times 10^{-3} M\left[1 + \left(\frac{M}{6380}\right)^{2.41}\right] \qquad (23)$$

which is the simple sum of two power laws, an empirical result which has also been found to apply for other polymers.[5] The intersection defines the characteristic molecular weight $M_c = 6.38 \times 10^3$ and the corresponding iso-free-volume kinematic viscosity $\nu_\infty(M_c) = 41.4$ St at 25 °C.

In the Rouse model expression for kinematic viscosity,

$$\nu = \frac{\zeta_0 N_a R_G^2}{6m_0} \qquad (24)$$

where N_a is Avogadro's number, m_0 is the monomer molecular weight ($m_0 = 54$ for polybutadiene), and ζ_0 is the monomeric friction coefficient. From dilute solution

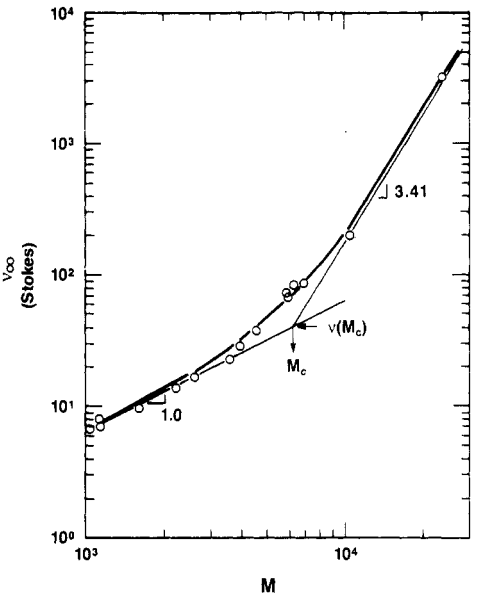

Figure 6. Kinematic viscosity vs. molecular weight for polybutadiene in the low molecular weight range. The data have been adjusted to the free volume state for high molecular weight polybutadiene at 25 °C as described in Appendix B.

measurements on similar polybutadiene samples at the Θ-condition,[29]

$$R_G^2 = 1.33 \times 10^{-17} M \quad (\text{cm}^2) \qquad (25)$$

This, together with eq 24, was used to obtain ζ_0 for high molecular weight polybutadiene at 25 °C from $\nu_\infty = 6.49 \times 10^{-3} M$, the low molecular weight asymptote of eq 23. The result is

$$\zeta_0 = 2.6 \times 10^{-7} \quad (\text{g s}^{-1}) \qquad (26)$$

This value is somewhat larger than $\zeta_0 = 1.1 \times 10^{-7}$ g s^{-1} obtained similarly by Roovers,[30] but the difference is due entirely to the free volume correction applied here. It is in reasonable accord with $\zeta_0 = 1.8 \times 10^{-7}$ g s^{-1} deduced from dynamic measurements in the transition region of lightly cross-linked low vinyl polybutadiene networks.[4] That estimate (see also ref 30) is based on the assumption that the Rouse model describes the high frequency response of long chains:[4]

$$G'(\omega) = G''(\omega) = \rho N_a R_G \left[\frac{\zeta_0 kT}{8m_0 M}\right]^{1/2} \omega^{1/2} \qquad (27)$$

where k is the Boltzmann constant. The prediction of eq 27 for $\zeta_0 = 2.6 \times 10^{-7}$ g s^{-1} is compared in Figure 7 with transition region data at $T_0 = 25$ °C. The shapes of $G'(\omega)$ and $G''(\omega)$ are certainly not Rouse-like; similar departures from the Rouse form are also found for other polymers.[4] All we can say is that the value of ζ_0 deduced from the viscosity for short chains is reasonably consistent with the location of the transition region for long chains. Values of ζ_0 deduced from the two regimes have been found to agree within a factor of about 3 in other polymer species.[4]

2. High Molecular Weight Polymers. Values of η_0 for samples with $M > 10^4$ were divided by M^3 and the results plotted as a function of M in Figure 8. By removing most of the molecular weight dependence in this way, we can observe departures from a nominal 3.4 power law more easily. Our results for $10^4 < M < 4 \times 10^5$ are fitted reasonably well by $\eta_0/M^3 \propto M^{0.4}$ as expected from eq 1, but they depart at higher molecular weights. Values of the exponent and prefactor obtained by power law fits over various ranges of molecular weight are given in Table

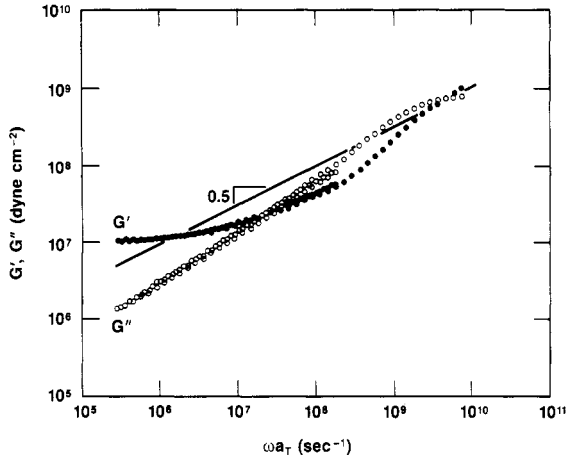

Figure 7. Dynamic storage and loss modulus in the transition region. Data for sample C20 at −76 °C and sample B2 at −76 and −86 °C are shown. Results for $|G^*| \gtrsim 10^9$ dyn/cm^2 may have been influenced by sample slippage (see text). The line represents the Rouse model prediction for $G'(\omega)$ and $G''(\omega)$ using the monomeric friction coefficient obtained from the viscosity of low molecular weight polybutadienes.

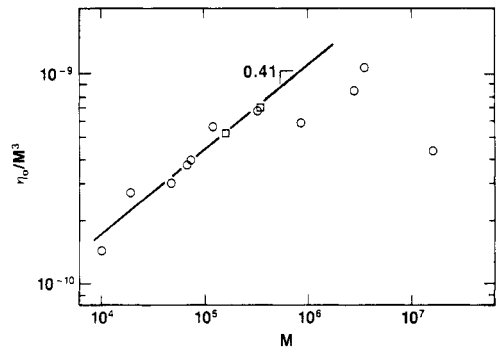

Figure 8. Viscosity reduced by the cube of molecular weight vs. molecular weight in the intermediate and high range. Molecular weights obtained from light scattering were used. The circles represent data for the samples prepared in this work; the squares represent data for the Roovers samples (Table XI).

Table XII
Values of Prefactor and Exponent in $\eta_0 = KM^a$ for the Polybutadiene Data in Table XI[a]

M range	no. of samples	$10^{11}K$ (P)	a	correlation coeff
10^4–10^5	8	0.316	3.43	0.9991
10^4–3.61 × 10^5	13	0.403	3.41	0.9995
10^4–4.41 × 10^5	14	0.572	3.37	0.9994
10^4–9.25 × 10^5	15	1.03	3.32	0.9991
10^4–3.74 × 10^6	16	1.29	3.30	0.9994
10^4–1.65 × 10^7	17	5.45	3.17	0.9984
3.55 × 10^5–3.74 × 10^6	5	4.18	3.21	0.9989
4.41 × 10^5–3.74 × 10^6	3	0.893	3.31	0.9995
4.41 × 10^5–1.65 × 10^7	4	115.0	2.96	0.9966
3.61 × 10^5–1.65 × 10^7	5	114.0	2.96	0.9975
3.55 × 10^5–1.65 × 10^7	6	112.0	2.96	0.9979
3.55 × 10^5–9.25 × 10^5	4	324.0	2.87	0.9990

[a] Data for sample B5 were omitted in these calculations because of its elevated vinyl content.

XII. The exponent decreases as samples beyond $M = 4 \times 10^5$ are included. The result for $10^4 < M < 3.61 \times 10^5$

$$\eta_0 = 4.0 \times 10^{-12} M^{3.41} \quad \text{(P)} \qquad (28)$$

agrees well with the data of Roovers[28] (adjusted to 25 °C) who also found reasonable agreement between his results and those from earlier polybutadiene studies.[31,32] Figure 9 is a similar plot using molecular weights obtained from $[\eta]$ in tetrahydrofuran (eq 9). The scatter is somewhat

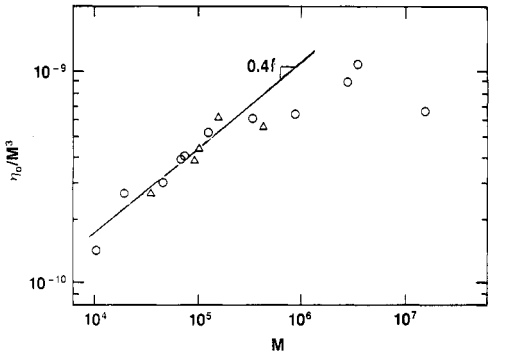

Figure 9. Viscosity reduced by the cube of molecular weight vs. molecular weight in the intermediate and high range. Molecular weights calculated from $[\eta]$ in tetrahydrofuran (eq 9) were used. The circles represent data for samples prepared in this work; the squares represent data for the Struglinski samples (Table XI).

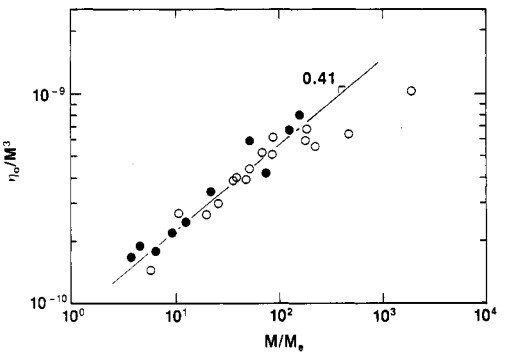

Figure 10. Viscosity reduced by the cube of molecular weight vs. molecular weight reduced by the entanglement molecular weight. The open circles represent polybutadiene data (samples B5 and B7 omitted); the filled circles represent data for fractions of polyisobutylene at 217 °C.[2] The polyisobutylene data have been shifted parallel to the η_0/M^3 axis into rough coincidence with the polybutadiene data.

reduced, but the same pattern of departures from $\eta_0 \propto M^{3.4}$ at high M is found.

A comparison with the melt viscosity behavior of polyisobutylene[2] is shown in Figure 10. Values of η_0/M^3 are plotted as a function of M/M_e ($M_e = 1.85 \times 10^3$ for polybutadiene[15] and 8.9×10^3 for polyisobutylene[4]). The polyisobutylene data have been shifted along the viscosity axis into rough agreement with those for polybutadiene. Data for samples B5 and B7 are not shown, the former because its elevated vinyl content might influence the behavior and the latter because the values of M and η_0 are known with less certainty. Polyisobutylene obeys the 3.4 power law over the full range of available data (up to $M/M_e = 1.6 \times 10^2$, which is also the approximate limit of data for other species[3]). The polybutadiene data extend about an order of magnitude beyond that, even with sample B7 omitted, and it is apparently in this range where departures from $\eta_0 \propto M^{3.4}$ begin to appear.

The validity of that conclusion depends of course on the accuracy of the molecular weight and viscosity measurements but also on the assumption that variations in polydispersity and cis–trans ratio are not important. We have already described our efforts to eliminate systematic errors in molecular weight (see Appendix A) and viscosity (see discussion of Table VIII). Judging by studies on mixtures,[4,15] our use of $\bar{M}_w$ should minimize effects due to polydispersity differences. From our SEC measurements, we know these differences are small up to $M \sim 10^6$, and we have some additional rheological assurance from the excellent superposability of $G^*(\omega)$ and of $G(t)$ for different samples in the terminal region[17,33] (including sample B6,

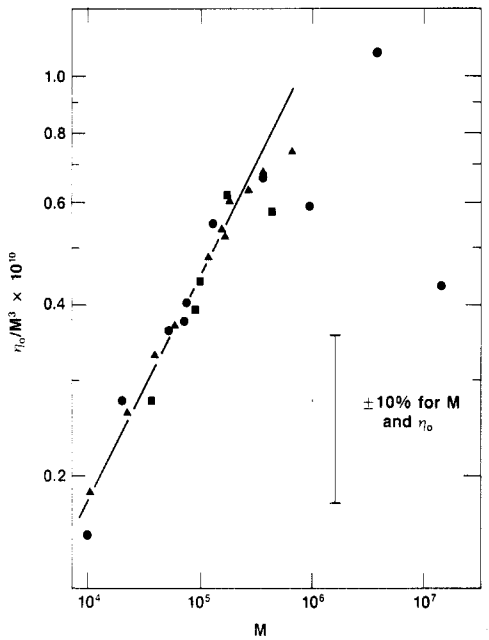

Figure 11. Viscosity reduced by the cube of molecular weight vs. molecular weight in the intermediate and high range. The circles represent data for samples prepared in this work (Table XI) with B5 omitted, the squares represent the Struglinski data (Table XI), and the triangles represent the data from Roovers[28] with viscosities adjusted to 25 °C. The line is eq 28.

$M = 3.74 \times 10^6$). On the other hand, the even more sensitive techniques of creep and creep recovery suggest that the polymers of highest molecular weight (samples B6 and B7) are more polydisperse than the others.[34] For those we must rely solely on our use of $\bar{M}_w$ to minimize the polydispersity effect, and we have in any case given somewhat less weight to the B7 results due to the difficulty of obtaining accurate values for such extremes of η_0 and $\bar{M}_w$.

Professor Plazek has pointed out to us the possibility of a more subtle problem in regard to sample B7, namely, that the polymer may not have reached an equilibrium state after being molded to form the creep test specimen. Such effects were found[35] in the ultrahigh molecular weight polystyrenes ($M = 4.4 \times 10^7$), but we think this is not a major factor in our case. Thus, a terminal relaxation time, $\tau_0 = \eta_0 J_e^0$, can be estimated from the recoverable shear compliance $J_e^0 \sim 1.7 \times 10^{-7}$ cm^2/dyn for narrow distribution polybutadiene[28] and $\eta_0 \sim 2.2 \times 10^{12}$ P for sample B7 at ambient conditions, giving $\tau_0 = 3.8 \times 10^5$s = 4.4 days. Polydispersity would certainly increase that value, but since the time between molding and testing was more than 1 month, the nonequilibrium effects should be small.

The possibility of systematic effects from the increase in cis–trans ratio with M seems unlikely but is difficult to rule out entirely. Two important determinants of viscosity are coil size and plateau modulus. Cis–trans ratio would appear to have little effect on R_G^2/M for polybutadiene over our range of compositions,[36] and the values of G_N^0 obtained for our samples[17,33] are independent of molecular weight through the range where the cis–trans ratio is changing most rapidly ($M \gtrsim 3 \times 10^5$). Although T_g and a_T also appear to be insensitive to cis–trans ratio in the intermediate range, the magnitudes of ζ_0 for cis and trans units might nevertheless be different. We have found no information in the literature to settle that question directly, but the results of Roovers[28] suggest strongly that the difference is negligible over our range of compositions. His samples were made in benzene and over the same range of molecular weights, $1 \times 10^4 < M < 3.6 \times 10^5$, have different cis–trans ratios (~1.3) than ours (~0.85), yet η_0/M^3

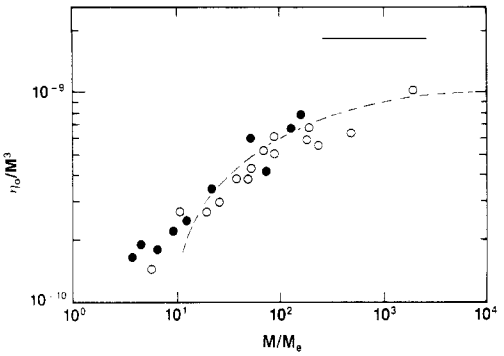

Figure 12. Same as Figure 10 with predicted reptation–tube-renewal asymptote (horizontal solid line) and estimated fluctuation contribution (dashed curve) given by eq 29 with $\mu = 1.7$.

vs. M for the two sets of samples agree very well. The comparison, with viscosities for the Roovers samples adjusted from 27 to 25 °C, is shown in Figure 11. Also included is a recently obtained result that was generously made available to us by Dr. Roovers: $\eta_0 = 3.75 \times 10^7$ P at 86.5 °C for a sample with $\bar{M}_w$(LS) = $7.6_0 \times 10^5$, corresponding to $\eta_0 = 3.4 \times 10^8$ P at 25 °C.

We estimate the error to be about 3% in both viscosity and molecular weight for $1 \times 10^4 < M < 5 \times 10^5$, which is roughly consistent with the scatter of results in that range (Figure 11). The uncertainties increase beyond that point and probably exceed 10% for sample B7. The errors from all sources seem too small to compromise our main conclusion of significant departure from the 3.4 power law at large M. The departures are not inconsistent with a limiting dependence of $\eta_0 \propto M^3$; the scatter is too large to justify a stronger statement.

The M^3 law is attractive on general grounds because it avoids the anomaly of unbounded increase in Λ (see eq 8). Also, $\eta_0 \propto M^3$ for sufficiently long linear polymers is an inevitable consequence of reptation theory,[13,37] and that theory accounts for many other features of entangled chain dynamics. Doi[38] has suggested that this law is approached from below as the result of a competing relaxation mechanism, path length fluctuations, whose contribution decreases slowly enough with increasing chain length to give the appearance of $M^{3.4}$ dependence in the usual experimental range. He proposed the following form in the intermediate region

$$\eta_0 = (\text{constant}) M^3 \left(1 - \mu \left(\frac{M_e}{M}\right)^{1/2}\right)^3 \qquad (29)$$

where μ is a constant of order unity. (Doi obtained $\mu = 1.47$ as the lower bound for a continuous Rouse chain.) Roovers[28] found that a smoothed version of this form with $\mu \sim 1$ gives a reasonable account of polybutadiene viscosities in the range $10^4 < M < 3.6 \times 10^5$. Lin has developed a similar relationship and tested it successfully with data for polystyrene melts.[39] In Figure 12 we have superimposed η_0/M^3 from eq 29 on our polybutadiene data (samples B5 and B7 omitted). An arbitrary vertical shift (choice of the proportionality constant) and horizontal shift (choice of μ) have been allowed to achieve a rough visual fit in the intermediate and high molecular weight ranges. The curve shown corresponds to $\mu = 1.7$ and an asymptotic limit of $\eta_0/M^3 \sim 1 \times 10^{-9}$ P.

The Doi–Edwards[13] theory gives an expression for the viscosity of linear polymers that relax by reptation alone. When written in terms of observables, the result is[40]

$$\frac{\eta_0}{M^3} = \frac{15}{4} \frac{(\eta_0/M)_R}{M_e^2} \qquad (30)$$

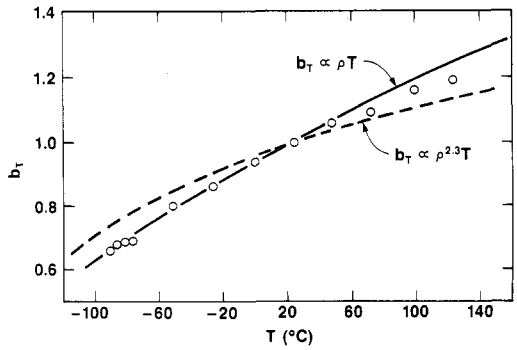

Figure 13. Modulus shift factor as a function of temperature (T_0 = 25 °C). Predicted forms based on eq 31 and 32 are shown.

where $(\eta_0/M)_R$ is the viscosity–molecular weight ratio of Rouse chains. With $M_e = 1.85 \times 10^3$ and the estimate $(\eta_0/M)_R = 6.49 \times 10^{-3}\rho = 5.8 \times 10^{-3}$ P from the small M asymptote of eq 23, we obtain $\eta_0/M^3 = 6.4 \times 10^{-9}$ P for pure reptation.

There is now considerable evidence that another relaxation mechanism, tube renewal, competes with reptation.[40] A model to describe that effect contains a universal constant z, the constraint release parameter.[41] The results of several types of experiments[6,12,40,42] are satisfied by $z \sim 3$, and for $z = 3$ the melt viscosities of monodisperse linear polymers are reduced from pure reptation values by the factor 0.30,[42] giving $\eta_0/M^3 = (0.30)\ (6.4 \times 10^{-9}$ P) $= 1.9 \times 10^{-9}$ P for the combination of reptation and tube renewal. That value, shown by the horizontal line in Figure 12, is within a factor of 2 of the estimated experimental asymptote of 1×10^{-9} P.

No great significance should be attached to the precise values obtained by such considerations, but they at least demonstrate consistency in magnitude with estimates based on some of the current ideas about the viscosity in entangled linear polymers. Many other theories have been proposed over the years, but a detailed discussion in light of eq 8 and our experimental results is beyond the scope of this work.

B. Modulus Shift Factor. In earlier work[19,23] the dependence of modulus shift factor on temperature for several species was compared with the classical form suggested by the Rouse model,[4]

$$b_T = \frac{\rho T}{(\rho T)_0} \tag{31}$$

and with another form suggested by simple dimensional arguments about the plateau modulus,[43]

$$b_T = \frac{\rho^d T C_\infty{}^{2d-3}}{(\rho^d T C_\infty{}^{2d-3})_0} \tag{32}$$

where $C_\infty(T)$ is the characteristic ratio of the species[44] and d is the exponent governing variations of plateau modulus with polymer concentration ($G_N^0 \propto c^d$). For polybutadiene, $d = 2.3$,[33] and we have taken the temperature coefficient of chain dimensions, $\mathrm{d} \ln C_\infty/\mathrm{d}T = \mathrm{d} \ln R_G^2/\mathrm{d}T = \kappa$, to be zero on the basis of measurements of $[\eta]$ vs. T in an oligomeric polybutadiene solvent.[45] The values of b_T in Table IX are compared with the two predictions in Figure 13. Densities at the various temperatures were calculated with the experimental values for high molecular weight polybutadiene obtained here, $\rho = 0.895$ g mL^{-1} at 25 °C and $\alpha = 7.0 \times 10^{-4}$ K^{-1}.

In contrast with the earlier results for other species,[19,23] the Rouse form (eq 31) describes b_T far better than eq 32. Roovers has also found good agreement with $b_T \propto \rho T$ for polybutadiene.[28] The data presented here were obtained at temperatures much closer to T_g than in the earlier studies; shift factors at the lower temperatures thus reflect behavior near or in the transition region, and the Rouse shift factor is probably more appropriate there. Indeed, $b_T \propto \rho T$ does not describe our high temperature data ($T > 25$ °C) as well, but on the other hand, $b_T \propto \rho^{2.3} T$ offers only a slight improvement. The molecular interpretation of b_T remains somewhat unsettled.

Table XIII
Second Virial Coefficients of Polybutadiene Samples in Cyclohexane

sample	$10^{-4}M$	$10^4 A_2$ (cm^3 g^{-1}) OP	$10^4 A_2$ (cm^3 g^{-1}) LS	$A_2M/[\eta]^a$
C18	2.00	16.4	14.9	0.76
CDS-30	4.60	25.0		
B1	7.09	13.2	12.7	0.97
C20	7.60	13.6		
B2	13.0	11.6	10.3	0.94
B3	35.5	9.2	8.5	1.02
C25	54.8		7.9	1.13
B4	92.5		6.7	1.10
B5	295		4.9	
B6	374		4.6	1.19
B7	1650		3.6	

[a] Calculated with values of A_2 from light scattering.

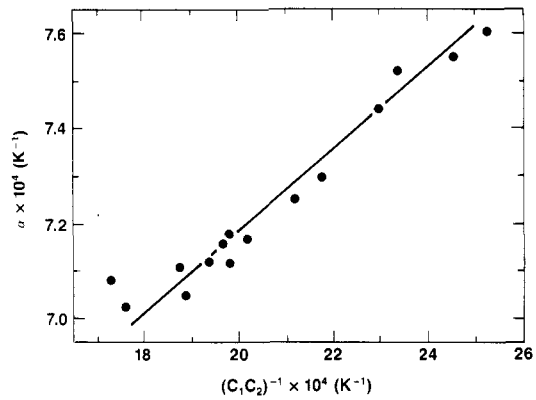

Figure 14. Relationship between thermal expansion coefficient and WLF coefficients. Line given by eq B-7 with $B = 0.20$ and $\alpha_s = 5.5 \times 10^{-4}$ K^{-1}.

Conclusions

We have found evidence for a systematic departure from the 3.4 power dependence of melt viscosity for linear polymers, beginning near $M/M_e = 200$. Viscosities lie consistently below the power law established with data on shorter but still well-entangled polymers. The results for higher molecular weights are too scattered to establish a clear form for the departure, but they are consistent with an approach to M^3 dependence. An η_0/M^3 asymptote estimated roughly from the data lies within a factor of 2 of a value calculated from reptation theory with the effects of tube renewal taken into account.

Acknowledgment. This work was supported by Exxon Research and Engineering Company through a grant to the Chemical Engineering Department of Northwestern University. We thank N. Hadjichristidis for invaluable assistance and advice on molecular characterization, D. S. Pearson for discussions about the rheological measurements, M. J. Struglinski and J. D. Tanzer for samples and data, and J. Roovers for samples, permission to use unpublished results, and numerous helpful comments. We are also grateful for the help of R. A. Casagrande with density measurements, K. R. Graf with FTIR, G. E.

Milliman with NMR, and W. M. Petrik with calorimetry. Finally, we acknowledge with gratidue the creep compliance results and critical comments provided by D. J. Plazek and D. L. Plazek.

Appendix A. Osmotic Pressure and Light Scattering Measurements

Reliability of molecular weights is obviously crucial in this study, so we describe our methods in some detail. Cyclohexane (Burdick & Jackson, distilled in glass) was the solvent used for both membrane osmometry (Wescan 230) and light scattering (Chromatix KMX-6, wavelength $\lambda = 633$ nm). Osmotic pressure π was measured at 32 °C for several concentrations in the dilute range (approaching overlap in some cases) and extrapolated to zero concentration to give

$$\bar{M}_n = RT/(\pi/c)_0 \tag{A-1}$$

where c is the polymer concentration (weight/volume).

Similarly, excess Rayleigh scattering ratio $\Delta R_\theta = R_\theta(c) - R_\theta(0)$ was measured at a small scattering angle θ for several concentrations in the dilute range (again approaching overlap in some cases) and extrapolated to zero concentration to give

$$\bar{M}_w = \frac{1}{K}\left(\frac{\Delta R_\theta}{c}\right)_0 \tag{A-2}$$

where K is the contrast factor,[46] equal to $8.29 \times 10^6 (dn/dc)^2$ cm^2 g^{-1} for cyclohexane (refractive index $n = 1.4254$ at $\lambda = 633$ nm). The refractive index increment dn/dc was determined for five samples (C19, B1, C25, B4, and B5) using four concentrations of each in a differential refractometer (Chromatix KMX-16). For all samples except B5, $dn/dc = 0.107 \pm 0.002$ mL g^{-1} was obtained. A smaller value, $dn/dc = 0.100$ mL g^{-1}, was obtained for sample B5, the difference being consistent with the elevated vinyl content[47] of that polymer.

The solvent and solutions for light scattering were clarified with Gelman Alpha-450 filters. Larger pore sizes were necessary for high molecular weight samples to avoid plugging and degradation; Nucleopore 12-μm filters were used for the highest molecular weight sample B7. Scattering intensity was usually measured only in the 6°–7° interval, but results at smaller scattering angles were found to be quite comparable, even for sample B7. Instrumental calibration was checked repeatedly by comparing solvent Rayleigh ratio with the value for cyclohexane[48] at $\lambda = 633$ nm, $R_\theta(0) = 5.3 \times 10^{-6}$ cm^{-1}.

Two extrapolation procedures were used to obtain $(\pi/c)_0$ and $(\Delta R_\theta/c)_0$ from measurements at finite concentration. Initial departures are governed by the second virial coefficient A_2

$$\frac{\pi}{cRT} = \frac{1}{\bar{M}_n} + A_2 c + \dots \tag{A-3}$$

$$\frac{Kc}{\Delta R_\theta} = \frac{1}{\bar{M}_w} + 2A_2 c + \dots \tag{A-4}$$

and linear extrapolations (π/c vs. c; $c/\Delta R_\theta$ vs. c) are certainly appropriate if the solutions are sufficiently dilute. However, curvature becomes appreciable as c approaches the overlap concentration $c^* \sim [\eta]^{-1}$, and measurements in this range were sometimes made necessary by limitations on the instrumental sensitivity ($\pi \gtrsim 0.5$ cm solvent for osmometry; $\Delta R_\theta/R_\theta(0) \gtrsim 0.3$ for light scattering). Curvature was less in square root plots ($(\pi/c)^{1/2}$ vs. c and $(c/\Delta R_\theta)^{1/2}$ vs. c), and some theoretical justification for such procedures has been offered.[49] The working equations are then

$$\left(\frac{\pi}{cRT}\right)^{1/2} = \frac{1}{\bar{M}_n^{1/2}} + \frac{A_2 \bar{M}_n^{1/2}}{2} c + \dots \tag{A-5}$$

$$\left(\frac{Kc}{\Delta R_\theta}\right)^{1/2} = \frac{1}{\bar{M}_w^{1/2}} + A_2 \bar{M}_w^{1/2} c + \dots \tag{A-6}$$

It is relatively easy to obtain accurate values of π at concentrations well below c^* if $\bar{M}_n$ is small enough (but still large enough that membrane permeation is not a problem). In that case, the values of $\bar{M}_n$ and A_2 obtained by either linear or square root plots are indistinguishable. It is also relatively easy to obtain accurate values of $\Delta R_\theta/R_\theta(0)$ at concentrations well below c^* if $\bar{M}_w$ is large enough, and again the choice of extrapolation procedure has little effect. Differences between results obtained by the two procedures appear in osmometry as $\bar{M}_n$ increases and in light scattering as $\bar{M}_w$ decreases: square-root plots give progressively smaller values of molecular weight than linear plots in both cases. The differences in our results were never very large (~15% at most) and grew smaller if data at the higher concentrations were omitted. From examination of data for all samples and comparisons with $\bar{M}_w/\bar{M}_n$ estimates from SEC, we concluded that square-root extrapolations were the most reliable in the awkward cases. Those results, obtained with somewhat less weight given to data at the higher concentrations, are reported in Table I. For sample B7, the reported value is the average of several independent sets of measurements whose results gave values of $\bar{M}_w$ ranging from 1.48×10^7 to 1.70×10^7.

The second virial coefficients obtained from osmometry and light scattering with the square-root analysis are listed in Table XIII. Values of A_2 for the same sample from the two types of experiments are certainly comparable, although those from light scattering appear to be consistently smaller by about 10%. The experimental values of $A_2 M/[\eta]$ for polybutadiene in cyclohexane (Table XIII) are typical of flexible linear chains in good solvents.[50]

Appendix B. Adjustment of Viscosity for Low Molecular Weight Polybutadienes to Constant Monomeric Friction Coefficient[3,4]

The viscosity of polymer liquids can be represented as the product of a friction coefficient ζ and a structural factor F:

$$\eta_0 = \zeta F \tag{B-1}$$

The structural factor for linear polymers depends on chain length but is insensitive to temperature. The friction coefficient, on the other hand, reflects the local dynamics and governs the temperature dependence of viscosity. It also depends on the concentration of chain ends, the effect of which vanishes with increasing molecular weight: $\zeta(M) = \zeta^\infty$ for long chains. The isothermal dependence of viscosity on molecular weight for short chain polymers is thus influenced by variations in both ζ and F. Viscosities must therefore be multiplied by the ratio ζ^∞/ζ in order to establish the dependence of F on M in the low molecular weight range.

We have used the idea that the friction coefficient for a homologous series depends only on f, the fractional free volume in the liquid, to obtain the adjustment factor ζ^∞/ζ for samples of low molecular weight polybutadiene. The procedure is first to obtain values of f_0, the fractional free volume at the reference temperature ($T_0 = 25$ °C), from the temperature dependence of viscosity, and then to calculate viscosities for the same polymers at f_0^∞, the free volume for high molecular polybutadiene at 25 °C. Thus, $\eta_0(f_0^\infty)/\eta_0(f_0) = \zeta^\infty/\zeta$ for each sample.

According to free volume theory, the viscosity of a liquid at any temperature T relative to its viscosity at a reference temperature T_0 is given by

$$\frac{\eta_0(f)}{\eta_0(f_0)} = \exp\left[B\left(\frac{1}{f} - \frac{1}{f_0}\right)\right] \tag{B-2}$$

where B is some constant of order unity. It is assumed that $f(T)$ is governed by the thermal expansion coefficient of free volume: $f = f_0 + \alpha_f(T - T_0)$. Equation 22 of the text then leads to

$$\log a_T = -\frac{(B/2.303f_0)(T - T_0)}{(f_0/\alpha_f) + T - T_0} \tag{B-3}$$

When the coefficients are equated with those in the WLF equation (eq 20), the the following relations are obtained:

$$f_0 = B/2.303C_1 \tag{B-4}$$

$$\alpha_f = B/2.303C_1C_2 \tag{B-5}$$

If B is independent of molecular weight in a homologous series, then eq B-2 and B-4 can be combined to give

$$\frac{\eta_0(f_0^\infty)}{\eta_0(f_0)} = \frac{\zeta^\infty}{\zeta} = \exp[2.303(C_1^\infty - C_1)] \tag{B-6}$$

where C_1^∞ designates the value of C_1 at high molecular weight. Equation B-6 was used with the values of C_1 in Table X to calculate ζ^∞/ζ for the low molecular weight polybutadienes at 25 °C. These results and the iso-free-volume values of kinematic viscosity ν_∞ are given in Table X.

The assumption of constant B within the series can be tested if it is further assumed that α_f is the difference between α for the liquid (eq 12) and some hard core solid value α_s which is independent of chain length. Equation B-5 then becomes

$$\alpha = \frac{B}{2.303}\frac{1}{C_1C_2} + \alpha_s \tag{B-7}$$

Accordingly, a plot of α vs. $(C_1C_2)^{-1}$ should be linear with slope $B/2.303$ and intercept α_s. The results fit the straight line form fairly well, as shown in Figure 14. However, the coefficients obtained, $B = 0.2$ and $\alpha_s = 5.5 \times 10^{-4}$ K^{-1}, are rather different from the more common values of $B \sim 1$ and $\alpha_s \sim 2 \times 10^{-4}$ K^{-1}, and $f_0^\infty = 0.025$ from eq B-4 is more typical of a polymer near T_g than one at $T + 125$ °C. It also seems contrary to free volume ideas that the Vogel temperature $T_\infty = T_0 - C_2$ and T_g move in opposite directions with increasing molecular weight: T_∞ increases with M, while T_g decreases with M (eq 13).

We have examined other methods to compensate for ζ variations, e.g., by comparing viscosities at constant $T - T_g$ or by imposing constant $T_g - T_\infty$ on the WLF correlations. The adjustment factors are somewhat different in those cases: ζ^∞/ζ is larger by factors of 2–3 at the lowest molecular weights. We settled for the method described above as being more widely practiced and slightly less arbitrary despite the atypical values of B and α_s that result. More detailed discussions about the limitations of free volume theory are given elsewhere.[17,51]

Registry No. Polybutadiene, 9003-17-2.

References and Notes

(1) Current address: Research Laboratories, Eastman Kodak Co., Rochester, NY 14650.
(2) Fox, T. G.; Flory, P. J. *J. Phys. Colloid Chem.* **1951**, *55*, 221.
(3) Berry, G. C.; Fox, T. G. *Adv. Polym. Sci.* **1968**, *5*, 261.
(4) Ferry, J. D. *Viscoelastic Properties of Polymers*, 3rd ed.; Wiley: New York, 1980.
(5) Graessley, W. W. *Adv. Polym. Sci.* **1974**, *16*, 1.
(6) (a) Green, P. F.; Mills, P. J.; Palmstrom, C. J.; Mayer, J. W.; Kramer, E. J. *Phys. Rev. Lett.* **1984**, *53*, 2145. (b) Green, P. F.; Kramer, E. J. *Macromolecules* **1986**, *19*, 1108.
(7) (a) Antonietti, M.; Coutandin, J.; Grütter, R.; Sillescu, H. *Macromolecules* **1984**, *17*, 798. (b) Antonietti, M.; Coutandin, J.; Sillescu, H. *Macromolecules* **1986**, *19*, 793.
(8) Bartels, C. R.; Crist, B.; Graessley, W. W. *Macromolecules* **1984**, *17*, 2702.
(9) Pearson, D. S.; VerStrate, G.; von Meerwall, E. D.; Schilling, F. C. *Macromolecules*, in press.
(10) Flory, P. J. *Faraday Disc. Chem. Soc.* **1979**, *68*, 14.
(11) Janeschitz-Kriegl, H. *Polymer Melt Rheology and Flow Birefringence*; Springer-Verlag: Berlin–Heidelberg, 1983.
(12) Bartels, C. R.; Crist, B.; Fetters, L. J.; Graessley, W. W. *Macromolecules* **1986**, *19*, 785.
(13) Doi, M.; Edwards, S. F. *J. Chem. Soc., Faraday Trans. 2* **1978**, *74*, 1802.
(14) Scher, H.; Shlesinger, M. F. *J. Chem. Phys.* **1986**, *84*, 5922.
(15) Struglinski, M. J.; Graessley, W. W. *Macromolecules* **1985**, *18*, 2630.
(16) Young, R. N.; Quirk, R. P.; Fetters, L. J. *Adv. Polym. Sci.* **1984**, *56*, 1.
(17) Colby, R. H. Doctoral Thesis, Chemical Engineering Department, Northwestern University, 1985.
(18) (a) Bahary, W. S.; Sapper, D. I.; Lane, J. H. *Rubber Chem. Technol.* **1967**, *40*, 1529. (b) Grebowicz, J.; Aycock, W.; Wunderlich, B. *Polymer* **1986**, *27*, 575.
(19) Carella, J. M.; Graessley, W. W.; Fetters, L. J. *Macromolecules* **1984**, *17*, 2775.
(20) Maekawa, E.; Mancke, R. G.; Ferry, J. D. *J. Phys. Chem.* **1965**, *69*, 2811.
(21) Colby, R. H.; Milliman, G. E.; Graessley, W. W. *Macromolecules* **1986**, *19*, 1261.
(22) Class, J. B., Hercules, Inc., private communication.
(23) Gotro, J. T.; Graessley, W. W. *Macromolecules* **1984**, *17*, 2767.
(24) Plazek, D. J. *J. Polym. Sci. A-2* **1968**, *6*, 621.
(25) Ninomiya, K. *J. Phys. Chem.* **1963**, *67*, 1152.
(26) Mohsin, M. A.; Berry, J. P.; Treloar, L. R. G. *Polymer* **1986**, *26*, 1463.
(27) Markovitz, H. *J. Polym. Sci., Polym. Symp.* **1975**, *50*, 431.
(28) Roovers, J. *Polym. J.* **1986**, *18*, 153.
(29) Hadjichristidis, N.; Zhongde, X.; Fetters, L. J.; Roovers, J. *J. Polym. Sci., Polym. Phys. Ed.* **1982**, *20*, 743.
(30) Roovers, J. *Polymer* **1985**, *26*, 1091.
(31) Gruver, J. T.; Kraus, G. *J. Polym. Sci. A* **1964**, *2*, 797.
(32) Rochefort, W. E.; Smith, G. G.; Rachapudy, H.; Raju, V. R.; Graessley, W. W. *J. Polym. Sci., Polym. Phys. Ed.* **1979**, *17*, 1197.
(33) Raju, V. R.; Menezes, E. V.; Marin, G.; Graessley, W. W.; Fetters, L. J. *Macromolecules* **1981**, *14*, 1668.
(34) Plazek, D. J.; Plazek, D. L., private communication.
(35) Plazek, D. J.; Raghupathi, N.; O'Rourke, V. M. *J. Polym. Sci., Polym. Phys. Ed.* **1980**, *18*, 1837.
(36) (a) Abe, Y.; Flory, P. J. *Macromolecules* **1971**, *4*, 219. (b) Tanaka, S.; Nakajima, A. *Polym. J.* **1972**, *3*, 500.
(37) (a) de Gennes, P. G. *J. Chem. Phys.* **1971**, *55*, 572. (b) de Gennes, P. G. *Scaling Concepts in Polymer Physics*; Cornell University: Ithaca, NY 1979.
(38) (a) Doi, M. *J. Polym. Sci., Polym. Lett. Ed.* **1981**, *19*, 265. (b) Doi, M. *J. Polym. Sci., Polym. Phys. Ed.* **1983**, *21*, 667.
(39) Lin, Y.-H. *Macromolecules* **1984**, *17*, 2846.
(40) Graessley, W. W. *Faraday Symp. Chem. Soc.* **1983**, *18*, 7.
(41) Graessley, W. W. *Adv. Polym. Sci.* **1982**, *47*, 67.
(42) Graessley, W. W.; Struglinski, M. J. *Macromolecules* **1986**, *19*, 1754.
(43) Graessley, W. W.; Edwards, S. F. *Polymer* **1981**, *22*, 1329.
(44) Flory, P. J. *Statistical Mechanics of Chain Molecules*; Wiley-Interscience: New York, 1969.
(45) Mays, J. W.; Hadjichristidis, N.; Graessley, W. W.; Fetters, L. J. *J. Polym. Sci., Polym. Phys. Ed.* **1986**, *24*, 2553.
(46) *Light Scattering from Polymer Solutions*; Huglin, M. B., Ed.; Academic: London, 1972.
(47) Chen, X.; Xu, Z.; Hadjichristidis, N.; Fetters, L. J.; Graessley, W. W.; Carella, J. M. *J. Polym. Sci., Polym. Phys. Ed.* **1984**, *22*, 777.
(48) Kaye, W.; McDaniel, J. B. *Appl. Opt.* **1974**, *13*, 1934.
(49) Casassa, E. F.; Berry, G. C. In *Polymer Molecular Weights*; Slade, P. E., Ed.; Marcel Dekker: New York, 1975; Part 1, Chapter 5.
(50) Yamakawa, H. *Modern Theory of Polymer Solutions*; Harper and Row: New York, 1971.
(51) Plazek, D. J. *J. Polym. Sci., Polym. Phys. Ed.* **1982**, *20*, 729.